Lubricating Oil Effects on the Transient Performance of a Turbocharged Diesel Engine

Evangelos G. Giakoumis[*]

Internal Combustion Engines Laboratory, Thermal Engineering Department,
School of Mechanical Engineering, National Technical Univ. of Athens,
9 Heroon Polytechniou Str., Zografou Campus, 15780, Athens, Greece

Abstract

The modeling of transient turbocharged diesel engine operation appeared in the early seventies and continues to be in the focal point of research, due to the importance of transient response in the everyday operating conditions of engines. The majority of research has focused so far on issues concerning thermodynamic modeling, as these directly affect performance and pollutants emissions. On the other hand, issues concerning the dynamics of transient operation are usually over-simplified, possibly for the sake of speeding up program execution time. In the present work, an experimentally validated transient diesel engine simulation code is used to study and evaluate the importance of the lubricating oil properties (oil-type, viscosity, temperature) on the transient response of a turbocharged diesel engine. It is revealed how the lubricating oil affects mechanical friction and hence, the speed response as well as the other interesting parameters, e.g. fuel pump rack position or turbocharger operating point for load-change schedules typical in the European Transient Cycles for heavy-duty engines. Particularly under low ambient conditions, the high oil viscosity is responsible for a significant increase in the respective frictional losses worsening the engine transient response.

Nomenclature

A   cross section area (m^2)

C   coefficient

D   cylinder bore (m)

[*] Tel.: +30 210 772 1360; fax: +30 210 772 1343.
E-mail address: vgiakms@central.ntua.gr (E.G.Giakoumis).

f	friction coefficient
F	force (N)
G	mass moment of inertia (kg m^2)
h	heat convection coefficient (W/m^{2}K)
h_{oil}	oil film thickness (μm)
k	thermal conductivity (W/mK)
L	thickness or length (m)
N	engine speed (rpm)
p	pressure (bar)
Q	heat loss (W)
r	crank radius (m)
s	Stribeck parameter
S	piston stroke (m)
t	time (sec)
T	temperature (^{o}C)
u	velocity (m/s)
V	volume (m^3)
w	width (mm)

Greek symbols

μ	dynamic viscosity (Ns/m^2)
ρ	density (kg/m^3)
τ	torque (Nm)
φ	crank angle (deg)
ω	angular velocity (rad/s)

Subscripts

c	coolant
cr	critical
e	engine
fr	friction
g	gas
gr	gravitational

in   inertia

L   load

pist   piston

pr   piston ring

T   torsional

w   wall

Abbreviations

°CA   degrees crank angle

bmep   brake mean effective pressure (bar)

bsfc   brake specific fuel consumption (g/kWh)

fmep   friction mean effective pressure (bar)

NEDC   new European Driving Cycle

rpm   revolutions per minute

TDC   top dead center

1. Introduction

The turbocharged diesel engine is nowadays the most preferred prime mover in medium and medium-large units applications. Moreover, it continuously increases its share in the highly competitive automotive market, owing to its reliability, which is combined with excellent fuel efficiency. Nonetheless, its transient operation, which comprises a significant portion of the everyday operating conditions of engines, is often linked with off-design (e.g. turbocharger lag) and consequently non-optimum performance and increased exhaust emissions. The latter points out the necessity for correct modeling of all individual engine processes.

During the last decades, diesel engine modeling has greatly supported the study of transient operation [1–5]. Ideally, a complete diesel engine transient simulation code should include analytical models for all thermodynamic and dynamic processes. However, when the main target of simulation is engine performance and pollutants emissions, which is actually the case in most research works, it seems reasonable to focus primarily on thermodynamics. In such cases, simplified approaches are usually

adopted for engine dynamic behavior in order to save execution time of the simulation code [3].

Engine friction is the most important of the above-mentioned dynamic issues. Frictional energy losses inside an internal combustion engine arise from the shearing of oil films between the various working surfaces, e.g. between piston rings and cylinder liner or inside the journal bearings; friction is, thus, interrelated with lubrication. Friction energy is ultimately removed as wasted heat by the cooling system of the engine. The interest for determining friction losses in engines has increased recently owing to the global requirements for lower fuel consumption and decreased CO_2 emissions, but also for increased engine durability [6].

It is a well known fact that friction torque varies significantly during the 720 °CA of a four-stroke engine cycle [7,8]; its magnitude compared to brake torque is not negligible, particularly at low loads where the most demanding transient events commence. Its modeling is, however, difficult due to the interchanging nature of lubrication (boundary, mixed, hydrodynamic) and the large number of components, i.e. piston rings, piston skirt, loaded bearings, valve train and auxiliaries that cannot be easily isolated, experimentally investigated, and studied separately even at steady-state conditions. Moreover, during transient operation, it has been argued that friction is characterized by non steady-state behavior, differentiating engine response and performance when compared to the corresponding steady-state values, i.e. at the same engine speed and fueling conditions. For example, Winterbone and Tennant [9] proposed that friction torque should be generally overestimated by some percentage points to account for the peculiarities during transients.

Friction modeling in transient simulation codes has, almost, always in the past been applied in the form of mean fmep relations, remaining constant for every degree crank angle in each cycle in the model simulation; thus, the effect of real friction torque on the model's predictive capabilities was limited. This is primarily attributed to the scarcity and complexity of detailed, per degree crank angle, friction simulations. It is also, probably, due to the fact that friction modeling does not affect heat release rate but only the crankshaft energy balance; the latter is, nonetheless, essential for correct transient predictions. Consequently, accurate friction modeling does not diversify engine thermodynamic properties and thus exhaust emissions. However, by defining

the magnitude of engine mechanical losses, it directly affects brake specific fuel consumption.

Past work by the present author research group [10,11], incorporating a fundamental friction model [12] in a transient simulation code, revealed that mean fmep modeling can underestimate the prediction of engine speed response by up to 8%.

The object of this paper is to expand on the previous research regarding friction development during transient operation by investigating the influence of oil-type and properties (temperature, viscosity). By so doing, ambient temperature effects are also taken under consideration, a fact that has not been accounted for in previous research studies but is nowadays an important aspect of the Certification of new vehicles (see, for example, the New European Driving Cycle for the homologation of new passenger cars, where the exhausts are sampled with the engine cold-started). To this aim, an experimentally validated, non-linear, transient diesel engine simulation code that follows the filling and emptying modeling technique is used [4,13]. Recently, a similar research was conducted on an experimental basis, alas for spark ignition engine and for steady-state only operation with similar results [14].

The results of the analysis are given in a series of detailed diagrams, which depict and quantify the effect of each oil parameter on the engine transient performance with special reference to the various friction terms (piston rings force, oil film thickness). Due to the narrow speed range of the engine in hand, only load increases under constant governor setting are investigated, which, nonetheless, play a significant role in the European Transient Cycles of heavy duty vehicles.

2. Simulation analysis

2.1 General process description

The present analysis does not, at the moment, include prediction of exhaust gas emissions and on the other hand deals with transient operation calculations on a °CA basis. Therefore, the simulation code that was developed in house follows the single-zone, filling and emptying approach, which is considered adequate for the thermodynamic processes evaluation. This approach has been shown to be the best

compromise between accuracy and limited PC program execution time [3,13]. The block diagram of the simulation code is depicted in Figure 1. The fuel is dodecane ($C_{12}H_{26}$) with a lower heating value of 42,500 kJ/kg. Perfect gas behavior is assumed. Polynomial expressions from Ref. [7] are used for each of the five species (O_2, N_2, CO_2, H_2O, and CO) considered, concerning the evaluation of internal energy and specific heat capacities for the first-law application to the engine cylinder contents.

For heat release rate predictions, the fundamental model proposed by Whitehouse and Way [15] is used. In this model the combustion process consists of two parts; a preparation limited combustion rate and a reaction limited combustion rate. Especially during transients, constant K in the (dominant) preparation rate equation of the model is correlated with the Sauter mean diameter (SMD) of the fuel droplets through a formula of the type $K \propto (1/SMD)^{2.5}$ [3]. For the evaluation of SMD (μm) an empirical expression proposed by Hiroyasu et al. [16] is used, namely, $SMD = 25.1\,(\Delta p)^{-0.135}\,\rho_g^{0.12}\,V_{tot}^{0.131}$ where Δp is the mean pressure drop across the injection nozzle in MPa (derived by the fuel pump sub-model discussed later in the text), ρ_g is the density of air in kg/m^3 at the time the injection starts, and V_{tot} is the amount of fuel delivered per cycle in mm^3 per pump stroke.

The simulation of heat loss Q_L to the cylinder walls is based on the improved model of Annand [17],

$$\frac{dQ_L}{dt} = A\left\{\frac{k_g}{D}Re^b\left[a(T_g - T_w) + \frac{a'}{\omega}\frac{dT_g}{dt}\right] + c(T_g^4 - T_w^4)\right\} \tag{1}$$

where a, a', b and c are constants evaluated after experimental matching at steady-state conditions. Further, $A = 2A_{pist} + A'$, with $A_{pist} = \pi D^2/4$ the piston cross section area and $A' = \pi D x$ with x the instantaneous cylinder height in contact with the gas. Also, T_g is the uniform gas temperature and $Re = \rho \bar{u}_{pist} D / \mu_g$ is the Reynolds number; $\bar{u}_{pist} = 2NS/60$ is the mean piston speed with S the piston stroke, and k_g, μ_g are the gas thermal conductivity and viscosity, respectively, expressed as polynomial functions of temperature T_g.

During transient operation, the thermal inertia of the cylinder wall is taken into account; this can be accomplished with the use of a heat transfer scheme, based on electrical circuit analogy that models the temperature distribution from the gas to the

cylinder wall up to the coolant as illustrated in Figure 2 [18]. By so doing the cylinder wall thickness, thermal conductivity and thermal diffusivity are taken into account. Applying the boundary conditions to all wall sides (gas side and coolant side) of a four-stroke diesel engine, the following equation is obtained

$$\frac{1}{4\pi} \int_0^{4\pi} \frac{dQ_L}{d\varphi} d\varphi = A \frac{k_w}{L_w} (\overline{T}_w - \overline{T}_{w,c}) = A h_c (\overline{T}_{w,c} - \overline{T}_c) \qquad (2)$$

where L_w is the cylinder wall thickness with k_w its thermal conductivity and h_c the heat transfer coefficient from the external wall side (respective mean temperature $\overline{T}_{w,c}$) to the coolant. Equations (2) are solved for the two unknown mean wall temperatures $\overline{T}_w$ and $\overline{T}_{w,c}$, which change from cycle to cycle during the transient event but they can be considered to remain constant throughout the cycle. Moreover, coolant temperature $\overline{T}_c$ changes according to the engine operation (cold starting, warm-up, fully-warmed-up conditions) and determines accordingly the (mean throughout an engine cycle) oil temperature T_{oil}.

As is the standard case in filling and emptying transient diesel engine simulation codes, the turbocharger is modeled based on its steady-state maps provided by the manufacturer. For the particular engine under study, the very high mass moment of inertia slows down considerably the whole transient event, prohibiting the turbocharger from very fast operating point changes and limiting the deviation of its transient operating point from the steady-state maps. Hence, it is felt that, for the current engine-load setup, the steady-state turbocharger modeling approach can be considered acceptable.

Moreover, the filling and emptying technique is extended to the simulation of the manifolds operation. Since the present engine is characterized by very small (exhaust) piping and the engine speeds under study are very low, it was not considered necessary to apply the very time-consuming method of characteristics for solving the governing equations of the unsteady flow in the pipes. It is strongly believed that, for the present engine, the above-mentioned assumption may only induce small errors in the model's predictive capability, as has already been discussed extensively in the past by the present research group [3,11,13].

Various sophisticated sub-models, which analyze important engine features during transient operation, have been incorporated in the main simulation code [3,4,11,13]; a few details are provided below.

Multi-cylinder engine modeling: At steady-state operation the performance of each cylinder of a multi-cylinder engine is practically the same, due to the practical fixed position of the mechanical fuel pump rack position, resulting in the same amount of fuel being injected per cycle, and the fixed turbocharger compressor operating point resulting in the same air mass flow–rate for each cylinder. On the other hand, under transient conditions each cylinder experiences different fueling and air mass flow–rate during the same engine cycle. This is the result of the combined effect of a) the continuous movement of the fuel pump rack, initiated by a load or speed change, and b) the continuous movement of the turbocharger compressor operating point. As regards speed changes, only the first cycles are practically affected, but, when load changes are investigated (as is the case with the present study), significant variations can be experienced throughout the whole transient event. The usual approach, here, is the solution of the governing equations for one cylinder and the subsequent use of suitable phasing images of this cylinder's behavior for the others. This approach is widely applied due to its low computational time. Unlike this, a 'true' multi-cylinder engine model is incorporated into the simulation code. Following this approach, all the governing differential and algebraic equations are solved separately for each cylinder, according to the current values of fuel pump rack position and turbocharger compressor air mass flow–rate. This causes significant differences in the behavior of each cylinder during the same transient cycle, affecting, among other things, engine response and exhaust emissions.

Fuel pump operation: Instead of applying the steady-state fuel pump curves during transients, a fuel injection model, experimentally validated at steady-state conditions, is used. Thus, simulation of the fuel pump–injector lift mechanism is accomplished, taking into account the delivery valve and injector needle motion. The unsteady gas flow equations are solved (for compressible injected fuel flow) using the method of characteristics, providing the dynamic injection timing as well as the duration and the rate of injection for each cylinder at each transient cycle. The obvious advantage here is that the transient operation of the fuel pump is also taken into account. This is

mainly accomplished through the fuel pump residual pressure value, which is built up together with the other variables during the transient event.

Friction: For the computation of friction torque, at each ^{o}CA, a detailed model is adopted, which describes the non-steady profile of friction torque during each cycle [12]. The total amount of friction is divided into four parts (piston rings assembly, valvetrain, loaded bearings and auxiliaries) with detailed per ^{o}CA equations for each of the above friction contributors. By so doing, variation of friction torque during an engine cycle (especially around 'hot' TDC) is established (Figure 3), unlike the usual 'mean fmep' approaches where friction torque is assumed constant throughout each transient cycle.

2.2 Crankshaft angular momentum equilibrium

The conservation of angular momentum applied to the total system (engine plus load), based on Newton's second-law of motion for rotational systems, is given by

$$\tau_e(\varphi,\omega) - \tau_{fr}(\varphi,\omega) - \tau_L(\omega) = G_{tot}\frac{d\omega}{dt} \tag{3}$$

where G_{tot} is the total mass moment of inertia of the system (engine–flywheel–brake) reduced on the crankshaft axis. The term $\tau_e(\varphi,\omega)$ represents the instantaneous engine indicated torque and includes gas, inertia and (the negligible) gravitational forces contribution; it is mostly dependent on accurate combustion modeling and is given explicitly by

$$\tau_e(\varphi) = \overbrace{\tau_g(\varphi)}^{Gas} + \overbrace{\tau_{in}(\varphi)}^{Inertia} + \overbrace{\tau_{gr}(\varphi)}^{Gravitational} = \left[p_g(\varphi)\cdot A_{pist}\cdot R_1(\varphi) + F_{Tin}(\varphi) + F_{gr}(\varphi) \right]\cdot r \tag{4}$$

where $p_g(\varphi)$ is the instantaneous cylinder pressure and $R_1(\varphi) = u_{pist}/r\omega$. For the calculation of inertia force F_{Tin}, a detailed model is applied treating the connecting rod as a rigid body experiencing reciprocating and rotating movement at the same time [10]. Also, $\tau_{fr}(\varphi,\omega)$ stands for the friction torque during transient operation and is modelled as analyzed in the previous subsection. Finally, $\tau_L(\omega)$ is the load torque, given by

$$\tau_L(\omega) = C_1 + C_2\omega^s \tag{5}$$

For a linear load-type (i.e. electric brake, generator) s=1, for a quadratic load-type (i.e. hydraulic brake, vehicle aerodynamic resistance) s=2, with C_1 the speed-independent load term (e.g. road slope for vehicular applications).

2.3 Oil properties

Oil viscosity μ_{oil} can be typically approximated by a Vogel type equation, i.e.

$$\mu_{oil} = C_1 \cdot e^{\left(\frac{C_2}{T_{oil}+C_3}\right)} \tag{6}$$

with C_1, C_2 and C_3 constants depending on the specific oil-type [19], and T_{oil} the mean, over an engine cycle, oil temperature in ^{o}C.

Figure 4 illustrates oil kinematic viscosity with respect to oil temperature for the various single- or multi-grade oil-types considered in the present analysis. Increase in oil temperature is generally desirable as it reduces considerably (logarithmically) the oil film viscosity, thus decreasing the amount of friction.

Closer examination of the curves in Figure 4 reveals that it is actually the low oil temperatures that differentiate remarkably in terms of oil viscosity; this trend is enhanced the higher the oil viscosity grade (grade number). On the other hand, the higher the oil temperature (i.e. for fully-warmed-up conditions), the smaller the observed difference between the various oil-types.

Figure 5 expands on the previous figure by illustrating typical oil temperature and viscosity variation during an engine cycle of the engine in hand. For oil temperature variation the experimental results from the analysis of Harigaya et al. [20] have been incorporated in the simulation code. In general, oil film temperature varies during an engine cycle about 5–10% around its mean value and so does oil viscosity following Eq. (6).

3. Experimental study

Prior to the parametric study, a detailed experimental investigation was carried out on a six-cylinder, turbocharged diesel engine with tight governing, operating under steady-state and transient conditions and running on SAE 30 oil. The basic data for the engine are given in Table 1.

The first requirement from the engine test bed instrumentation was to investigate the steady-state performance of the examined engine. For this purpose, an extended series of trials was conducted in order on the one hand to examine the model's predictive capabilities and on the other to calibrate successfully the individual sub-models. Figure 6a shows the comparison between experiment and simulation for the whole engine speed operating range and for various loads. Brake mean effective pressure (bmep), brake specific fuel consumption (bsfc), boost pressure, and turbocharger speed are depicted in this figure. It is obvious that the matching between experimental and simulated results is satisfactory for all engine operating conditions, providing a sound basis for the transient study by successfully calibrating the heat release, heat transfer etc sub-models. Figure 6b expands on the previous figure by showing two typical experimental vs. predicted cylinder pressure diagrams for representative engine operating conditions.

For the transient tests conducted, the initial speed was 1180 or 1380 rpm, and the initial load 10% of the engine full load. The final conditions for the transient events varied from 47 to 95% of the engine full load [4]. A typical example of a transient experiment is given in Figure 7, showing the response of some important engine and turbocharger properties. Here, the initial load was 10% of the full engine load at 1180 rpm. The final load applied was almost 50% of the full engine load (400% relative load-change). The overall matching between experimental and predicted transient response seems fairly satisfactory for both engine and turbocharger variables as regards trends and final operating conditions of the engine. Boost pressure is delayed compared to the speed profile owing to the well known turbocharger lag effect, which, for the particular engine-brake setup, was less pronounced due to the relatively high mass moment of inertia.

Some remarks concerning the matching between predicted and experimental transient results are provided below. The application of the final load was effected by the movement of the brake control lever (this task lasted 0.2 s), which in turn increased the amount of water inside the brake, by appropriately increasing the active surface of the inlet tube. Unfortunately, the hydraulic brake used in the experimental procedure is characterized by a high mass moment of inertia, of the order of 5.375 kgm^2, resulting in long, abrupt and non-linear actual load-change profile. The actual duration of the load application was accounted for in the simulation model by

increasing the load application time. The non-linear character of the load application though, which could not be accounted for in the simulation, is responsible for the (small) differences observed between experimental and simulated results in Figure 7.

4.   Results and discussion

Figure 8 illustrates a typical load increase transient event of the order of 10–75% commencing from an engine speed of 1180 rpm; this is the baseline for the analysis that follows. Engine speed, fuel pump rack position and boost pressure response are depicted for fully warmed-up (i.e. oil and coolant temperature at 90°C) engine conditions and for the various oil-types investigated.

The influence of oil temperature and type on the transient engine performance derives from its effect on the friction torque as indicated in Eq. (3). The important finding from Figure 8 is the fact that the specific oil-type seems to play a rather minor role in the engine transient response when operating at fully warmed-up conditions (differentiation of engine properties response after the 40th cycle is a matter of specific governor characteristics). Recall that from Figure 4, only the low oil temperatures were found to affect significantly the oil viscosity. Hence, for fully warmed-up conditions, the friction torque term in Eq. (3) differentiates only marginally producing the rather negligible response differences in Figure 8.

The next logical step is to investigate the effect of oil-type for lower than 90°C temperatures on the engine transient response; this is actually accomplished in Figure 9. Consistent with the results of Figure 4, oil viscosity differentiates the lower the oil temperature affecting accordingly the engine speed response as well as the other engine and turbocharger variables that are not depicted in Figure 9. The increase in oil viscosity with lower temperatures is reflected into higher friction torque terms $\tau_{fr}(\varphi)$, hence larger torque deficit during the early cycles leading to greater speed droops (droop is defined as the (maximum or final) speed change divided by initial speed) and advancing slightly the cycle where the instantaneous maximum speed droop is observed; recovery period on the other hand seems to remain unaffected but this is a rather unique characteristic of the engine under study, which is characterized by a high total moment of inertia and tight governing.

The above remarks are expanded in Figure 10, which illustrates engine speed response for various oil-types and oil temperatures. Again, from Figure 4, the higher the oil-grade number the greater the oil viscosity differences at low ambient (and oil) temperatures. As a result even greater speed droops (e.g. 95 rpm or 8% of the initial engine speed for SAE 50 oil at 30°C compared to 36 rpm or 3% for the nominal case – that is a remarkable 166% increase) are experienced compared to the results of Figures 8 and 9.

In order to analyze in more detail the latter findings, Figure 11 is provided that quantifies an important engine friction term during the transient event, namely piston ring assembly friction. An important aspect of friction theory is the mode of lubrication, which can be hydrodynamic, mixed or boundary. In hydrodynamic friction, the surfaces are separated by a liquid film, minimizing the respective wear. This is the desired lubrication mode during engine operation. As pressure increases or speed decreases, oil film thins out to the point where its thickness is comparable in size to the surface irregularities. This is the mixed lubrication regime. With further increase in load or decrease in speed, the boundary layer regime is reached, which, for internal combustion engine applications, is experienced, for example, around dead centers for piston rings. For most part of the piston stroke, lubrication is hydrodynamic, with metal contact occurring near firing TDC. The duty parameter s of the typical Stribeck diagram is defined as [7,12]

$$s = \frac{\mu_{oil}\left|u_{pist}\right|}{F_{ring}/L_{ring}}$$
(7)

with L_{ring} the active length of the ring profile, and F_{ring} the normal force of the ring profile, which is the sum of the ring diametral elastic tension and the instantaneous force from the gas pressure inside the cylinder. For hydrodynamic lubrication (s>s_{cr}), the friction coefficient is [12]

$$f_{pr} = C_4 \cdot s^{c_5}$$
(8a)

whereas, for the mixed lubrication regime (s<s_{cr}), it is given by

$$f_{pr} = f_o\left(1 - \frac{s}{s_{cr}}\right) + f_{cr}\frac{s}{s_{cr}}$$
(8b)

with f_o=0.28, s_{cr}=0.00001 (for cast iron), and $f_{cr} = C_4 \cdot s_{cr}^{c_5}$.

The corresponding piston ring friction force is then

$$F_{pr} = f_{pr}F_{ring} \qquad (9)$$

and is illustrated in Figure 12 for an early cycle of the examined transient event.

Piston rings friction force increases considerably the lower the oil temperature owing to the high μ_{oil} values as dictated by Eq. (6). On the other hand, piston rings friction force decreases with a decrease in engine speed due to the lower u_{pist} values. For the examined transient event, however, the effect of engine speed is minimal owing to the small speed droop observed; hence it is the oil temperature that primarily determines the piston ring friction force development (Figure 12). Since piston rings assembly for the present engine assumes at least 50% of the total friction torque, it is not surprising that the engine speed response worsens considerably with lower temperatures and higher oil-grade numbers. On the other hand, the greater the instantaneous speed droop the larger the displacement of the fuel pump rack and the higher the fueling during the transient event (Figure 11). The above remarks are expected to affect crankshaft deformation and stress owing to the higher cylinder pressures originating from the increased fueling.

Oil film thickness between ring and cylinder liner, on the other hand, is given by [12]

$$h_{oil} \cong w_{ring}s \qquad (10)$$

and is also illustrated in Figure 12 for an intermediate transient cycle. An approximation sign is used in Eq. (10) since at the dead centres, where the piston velocity is zero, oil film thickness 'h_{oil}' is not zero due to oil squeeze effects. Similar remarks, as the ones discussed for piston ring friction force, hold for the mean value, over each engine cycle, of the upper piston ring oil film thickness (demonstrated in Figure 13); the latter is governed by the oil viscosity through the Stribeck variable 's' but is also influenced by the instantaneous cylinder pressures. A decreasing (mean) oil film thickness trend is observed throughout the transient event, owing to the harder push of the ring against the liner that originates from the increasing fueling/gas pressures following the higher loading. On the other hand, for cold ambient conditions, oil film is significantly thicker (at least one order of magnitude higher for cold starting conditions compared to fully warmed-up operation) affecting accordingly friction force and engine speed droop, as the available net (indicated minus friction) engine torque is lower. The significant amount of friction torque for the SAE 50 oil at 30°C is

responsible for the rather unique trend observed during the first cycles in Figures 11 and 13 compared to the other examined cases.

5. Error analysis

In order to assess the sensitivity of the model calculations to uncertainties of input variables, a parametric computational study is performed. The values of oil temperature and kinematic oil viscosity at the nominal transient load case (10–75% load increase, engine running on SAE 30 oil) are varied throughout their possible ranges, which are indicated by the accuracies of the relevant measuring devices. Table 2 shows the respective values and relative errors of the maximum and final speed droop calculated by the model. For all possible cases, it is clear that the relative error in both maximum and final speed droop is always less than 1%. As regards the computational crank angle step used for the integration of the various differential equations of the model, it was found that the precision of solution was not influenced for values less than 1 ^{o}CA. Finally, the accuracy range investigated (from 0.001% to 0.1%) for convergence of a variable between two successive iterations did not affect the computational time required or the calculated values themselves.

6. Conclusions

An experimentally validated simulation code has been used to study the effect of oil-type and properties on a tight-governed turbocharged diesel engine transient response after a ramp increase in engine load. For the present engine–load configuration analysis, it was revealed that the lower the oil temperature and the higher its grade number the higher its kinematic viscosity hence piston rings friction force and total friction torque. Consequently, the transient load increase event is characterized by larger speed droop, larger displacement of the fuel pump rack position and ultimately higher crankshaft stress; likewise, the exhaust emissions are strongly influenced as was recently established based on both simulation [21] and experimental investigation at the author's laboratory on a similar engine.

References

[1] Watson N. Eliminating rating effects on turbocharged diesel engine response. SAE Paper no. 840134, 1984.

[2] Filipi Z, Wang Y, Assanis D. Effect of variable geometry turbine (VGT) on diesel engine and vehicle system transient response. SAE Paper no. 2001-01-1247, 2001

[3] Rakopoulos CD, Giakoumis EG. Review of thermodynamic diesel engine simulations under transient operating conditions. SAE Paper no. 2006-01-0884, SAE Trans, J Engines 2006;115:467-505.

[4] Rakopoulos CD, Giakoumis EG, Hountalas DT, Rakopoulos DC. The effect of various dynamic, thermodynamic and design parameters on the performance of a turbocharged diesel engine operating under transient load conditions. SAE Paper no. 2004-01-0926, 2004.

[5] Winkler N, Angström H-K. Simulations and measurements of a two-stage turbocharged heavy-duty diesel engine including EGR in transient operation. SAE Paper no. 2008-01-0539, 2008.

[6] McGeehan JA. Literature review of the effects of piston ring friction and lubricating oil viscosity on fuel economy. SAE Paper no. 780673, 1978.

[7] Ferguson CR, Kirkpatrick A. Internal combustion engines: applied thermo-sciences, 2nd edition. New York: Wiley, 2001.

[8] Ciulli E. A review of internal combustion engine losses, Pt. 2: studies for global evaluations. Proc Inst Mech Engrs, J Automobile Engng 1994;207:229-40.

[9] Winterbone DE, Tennant DWH. The variation of friction and combustion rates during diesel engine transients. SAE Paper no. 810339, 1981.

[10] Rakopoulos CD, Giakoumis EG, Dimaratos AM. Evaluation of various dynamic issues during transient operation of turbocharged diesel engine with special reference to friction development. SAE Paper no. 2007-01-0136, 2007.

[11] Rakopoulos CD, Giakoumis EG. Diesel engine transient operation. London: Springer-Verlag, 2009.

[12] Taraza D, Henein N, Bryzik W. Friction losses in multi-cylinder diesel engines. SAE Paper no. 2000 01-0921, 2000.

[13] Rakopoulos CD, Giakoumis EG. Sensitivity analysis of transient diesel engine simulation. Proc Inst Mech Engrs, J Automobile Engng 2006;220:89-101.

[14] Skjoedt M, Butts R, Assanis DN, Bohac SV. Effects of oil properties on spark-ignition engine friction. Tribilogy Int 2008;41:556-63.

[15] Whitehouse ND, Way RGB. Rate of heat release in diesel engines and its correlation with fuel injection data. Proc Inst Mech Engrs 1969-70;184:17-27.

[16] Hiroyasu H, Kadota T, Arai M. Development and use of a spray combustion modelling to predict diesel engine efficiency and pollutant emissions. Bulletin JSME 1983;26:569-576.

[17] Annand WJD, Ma TH. Instantaneous heat transfer rates to the cylinder head surface of a small compression ignition engine. Proc Inst Mech Engrs 1970-71;185:976-987.

[18] Rakopoulos CD, Giakoumis EG, Rakopoulos DC. Study of the short-term cylinder wall temperature oscillations during transient operation of a turbocharged diesel engine with various insulation schemes. Int J Engine Res 2008;9:177-93.

[19] Cameron A, Ettles CCMc. Basic lubrication theory, 3rd edition. Chichester UK: Ellis Horwood Ltd, 1981.

[20] Harigaya Y, Suzuki M, Takiguchi M. Analysis of oil film thickness on a piston ring in diesel engine: effect of oil film temperature. Trans ASME, J Engng Gas Turbines Power 2003;125:596-603.

[21] Rakopoulos CD, Dimaratos AM, Giakoumis EG, Rakopoulos DC. Evaluation of the effect of engine, load and turbocharger parameters on transient emissions of a diesel engine. Energy Convers Manage (submitted for publication)

Figures Captions

Figure 1: Block diagram of transient simulation code

Figure 2: Schematic arrangement of cylinder heat transfer scheme

Figure 3: Friction torque variation at initial and final cycle of a 10-75% load increase transient event - comparison between analytical and constant fmep modeling.

Figure 4: Kinematic viscosity vs. oil temperature for various oil-types.

Figure 5: Variation of oil temperature and viscosity during the initial cycle of the 10-75% load increase transient event for fully warmed-up conditions.

Figure 6a: Experimental and predicted engine and turbocharger steady-state results for the whole engine operating range

Figure 6b: Comparison between measured and predicted cylinder pressure diagrams, for two typical engine operating conditions.

Figure 7: Experimental and predicted engine transient response to an increase in engine load for SAE 30 oil operation and fully warmed-up conditions.

Figure 8: Engine response after a 10-75% load increase for various oil-types at fully warmed-up conditions.

Figure 9: Engine speed response during a 10-75% load increase transient event for SAE 30 oil at various temperatures.

Figure 10: Engine and turbocharger properties response during a 10-75% load increase transient event for various oil-types and temperatures.

Figure 11: Piston ring assembly fmep response during a 10-75% load increase transient event for various oil-types and temperatures.

Figure 12: Variation of upper piston ring friction force and oil film thickness during an early cycle of the 10-75% transient event.

Figure 13: Upper piston ring mean oil film thickness during a 10-75% load increase transient event for various oil-types and temperatures.
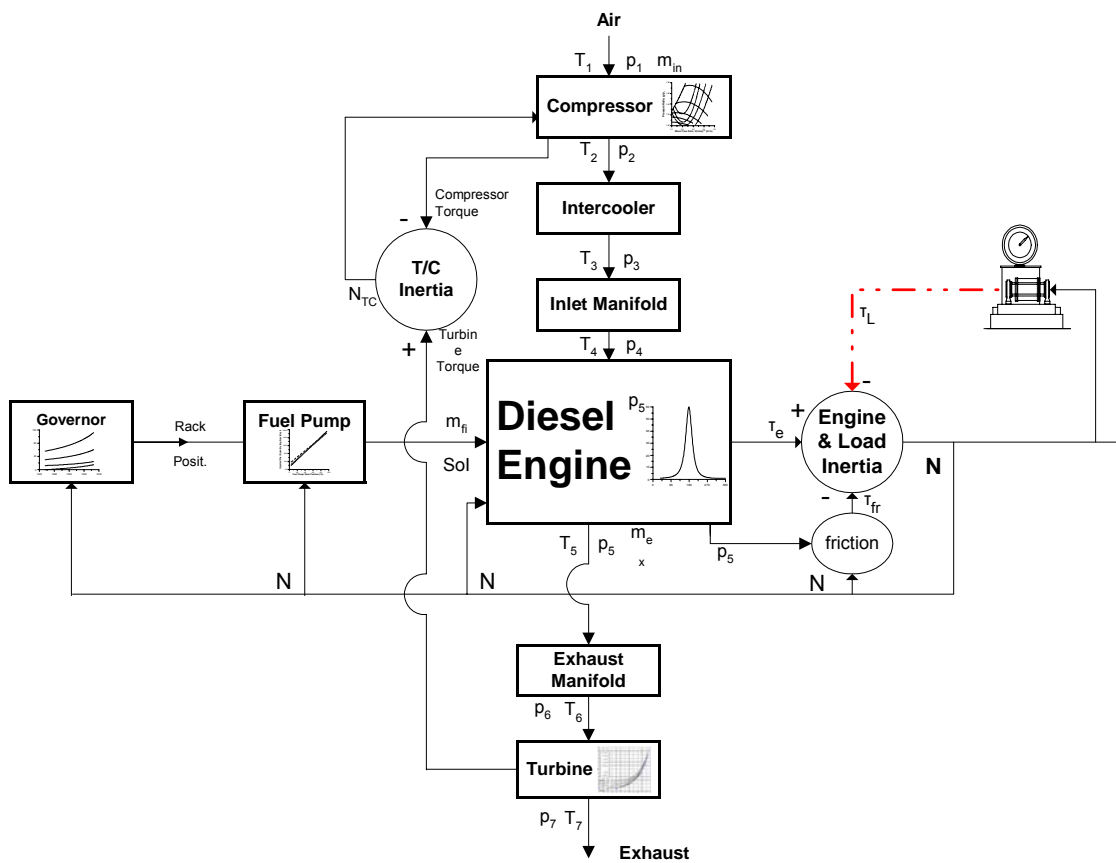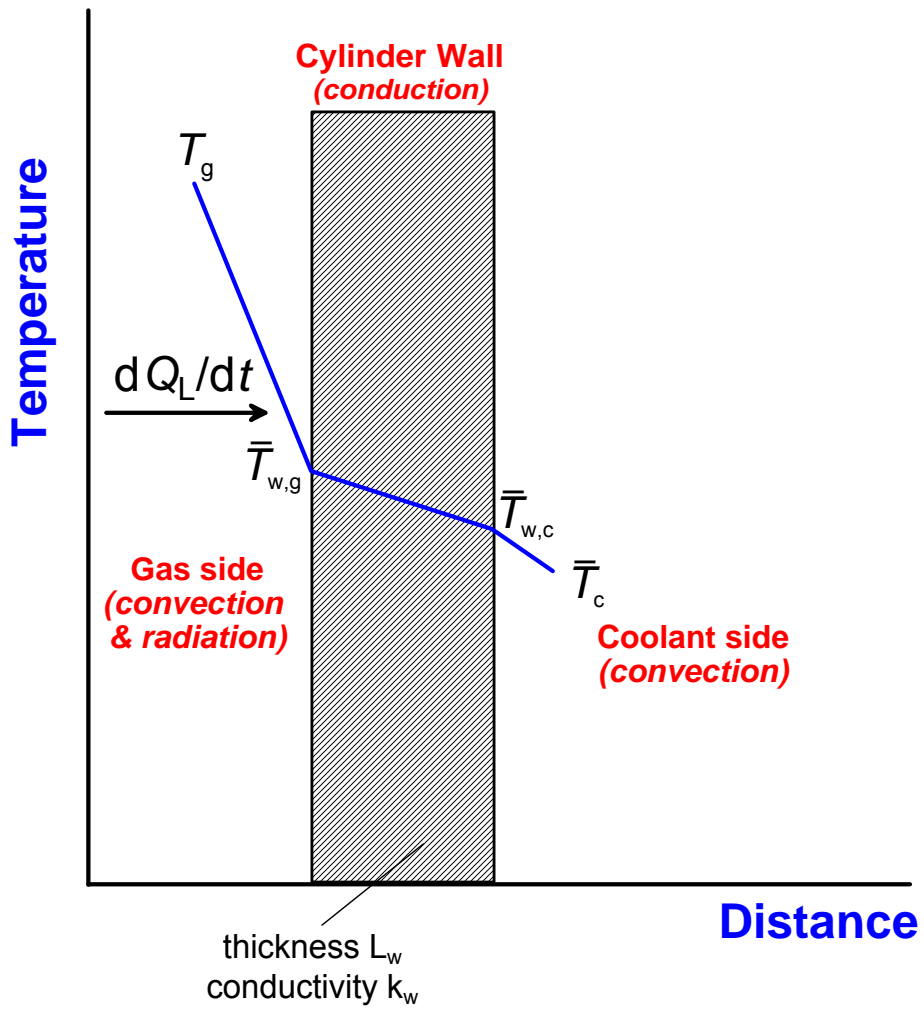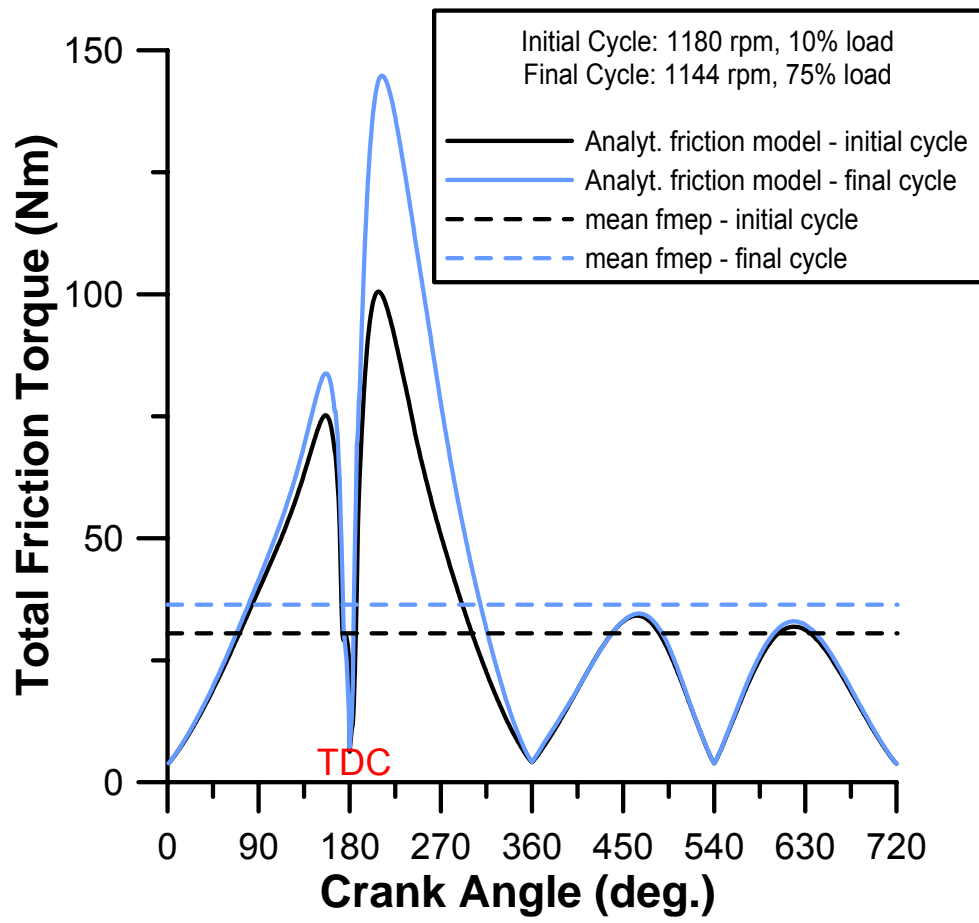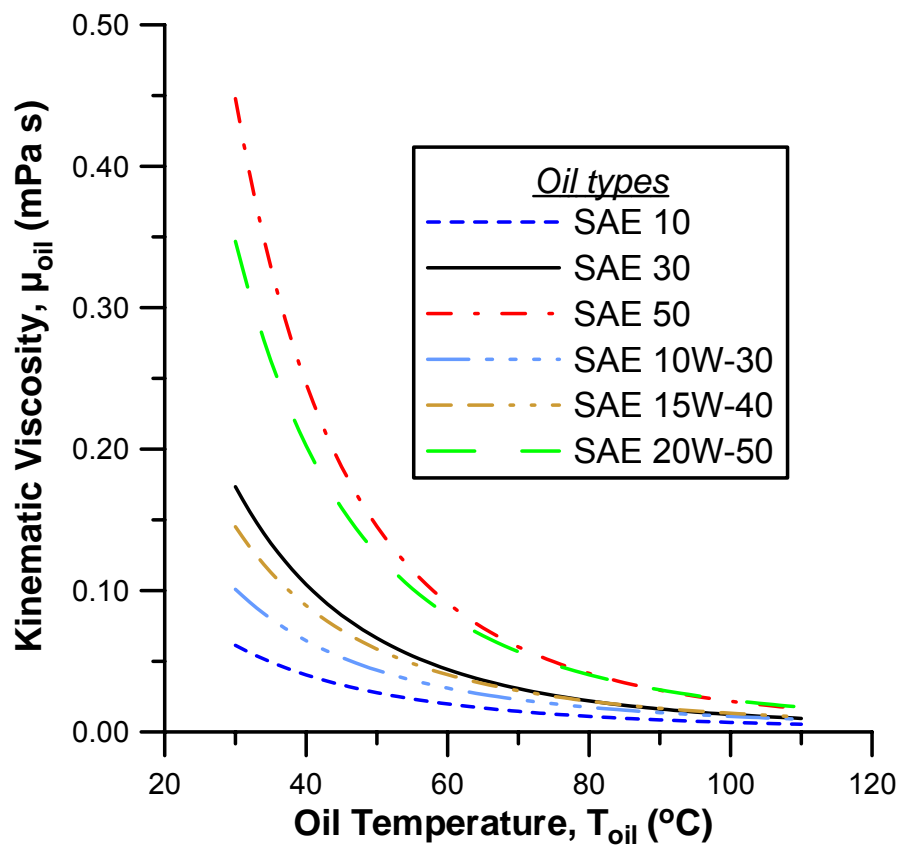
Figure 1

Figure 2

Figure 3

Figure 4
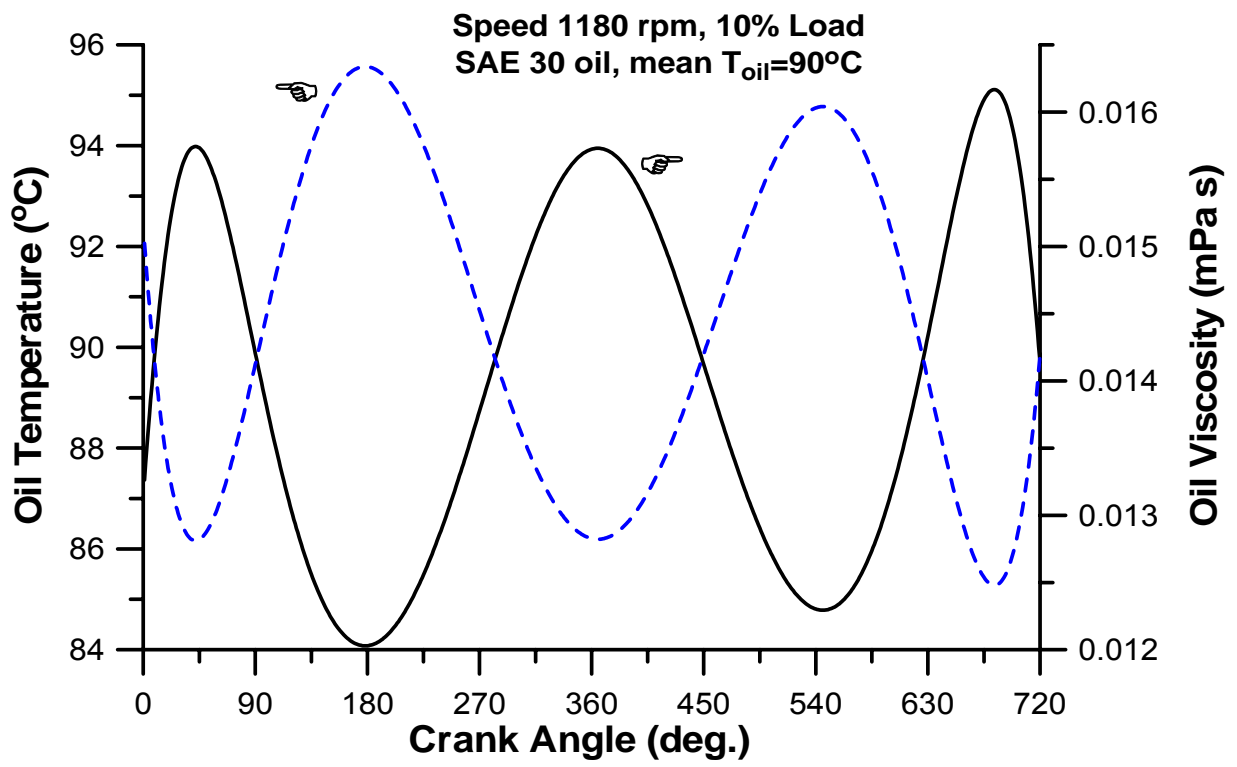
Figure 5
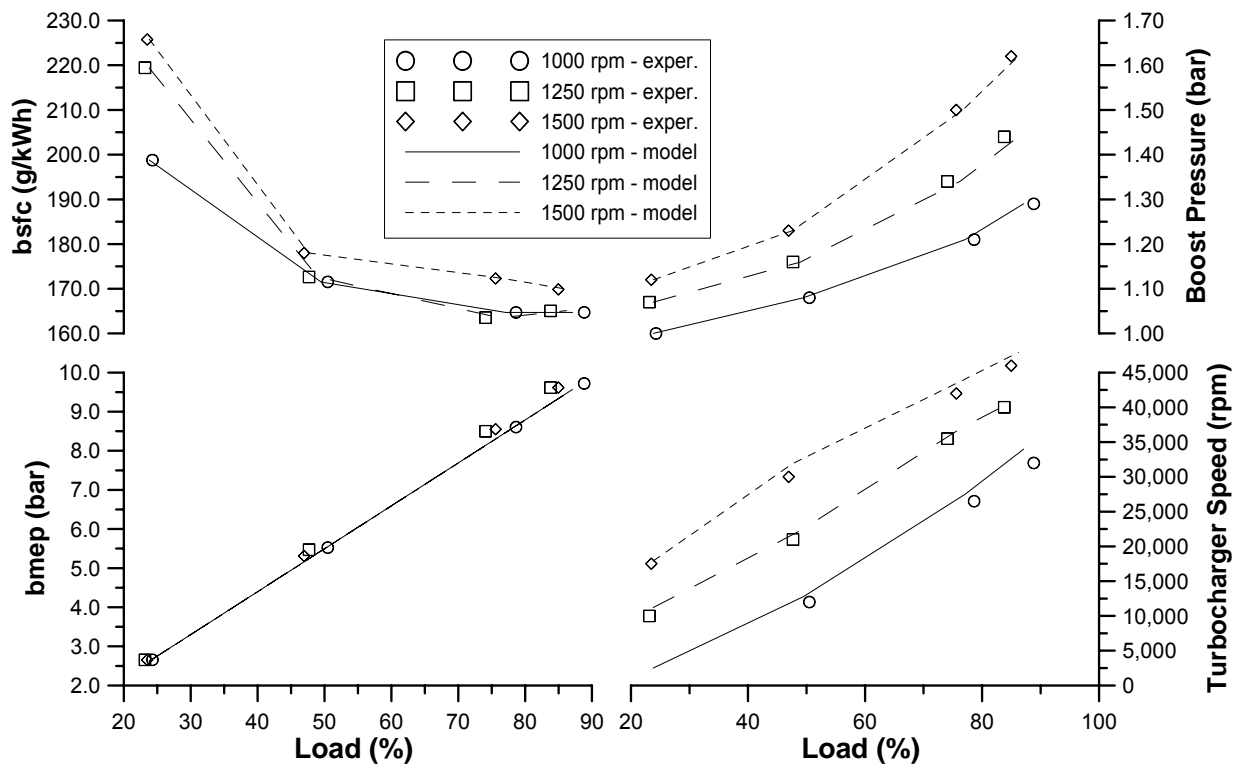
Figure 6a
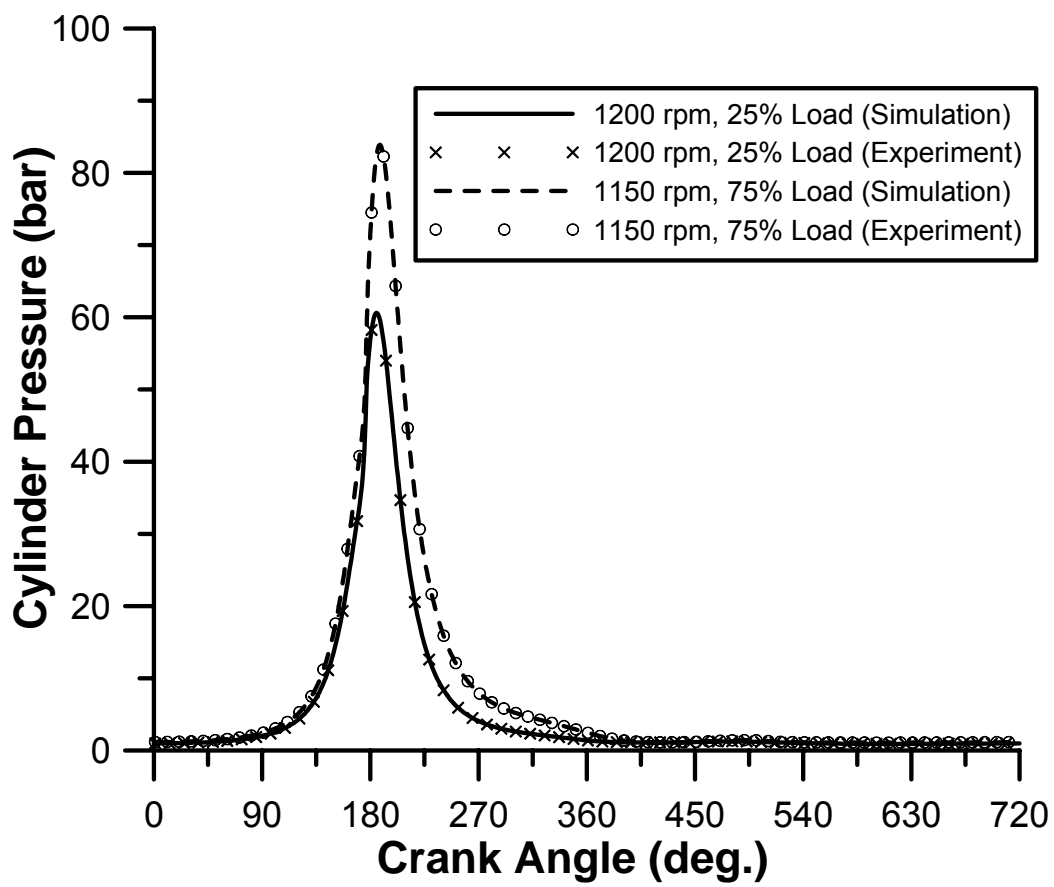
Figure 6b
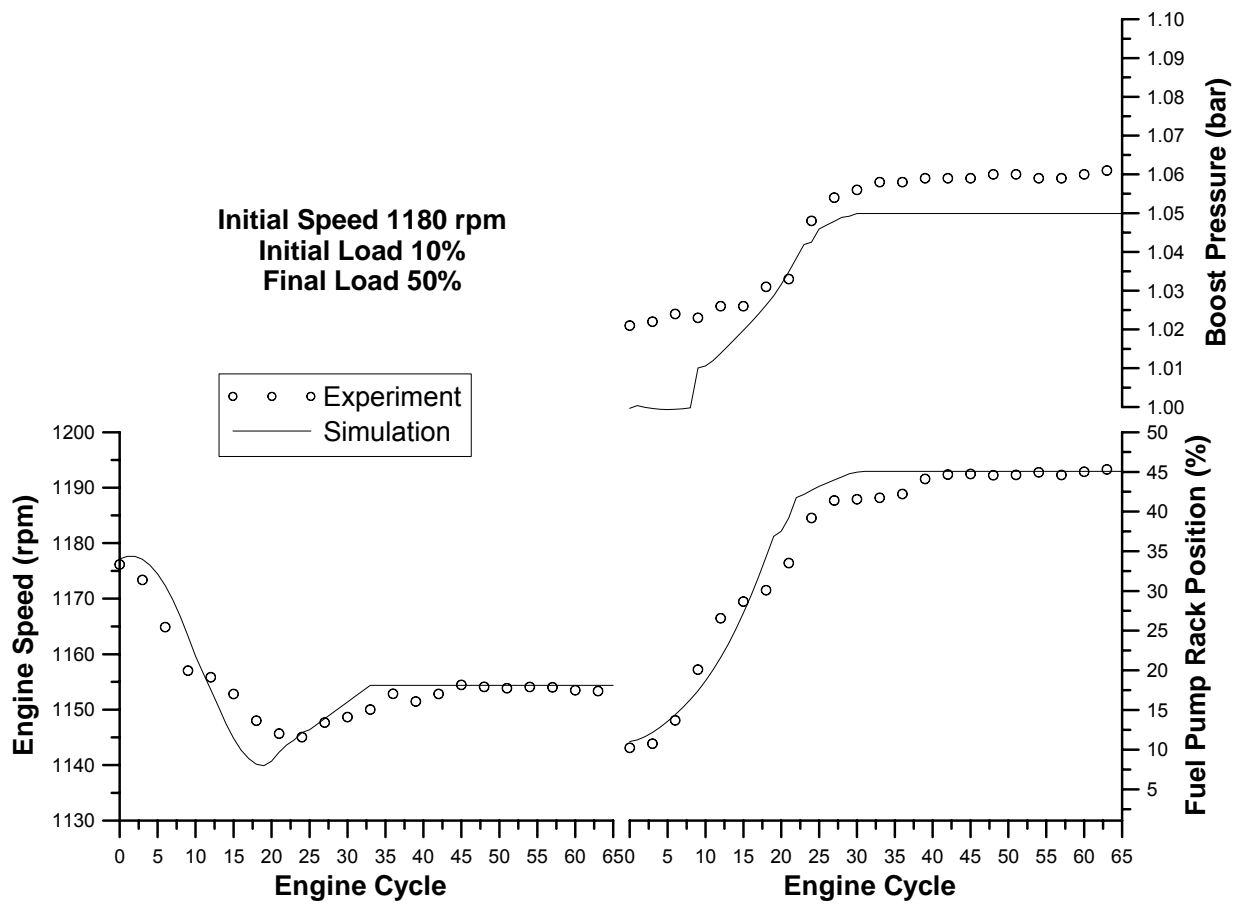
Figure 7
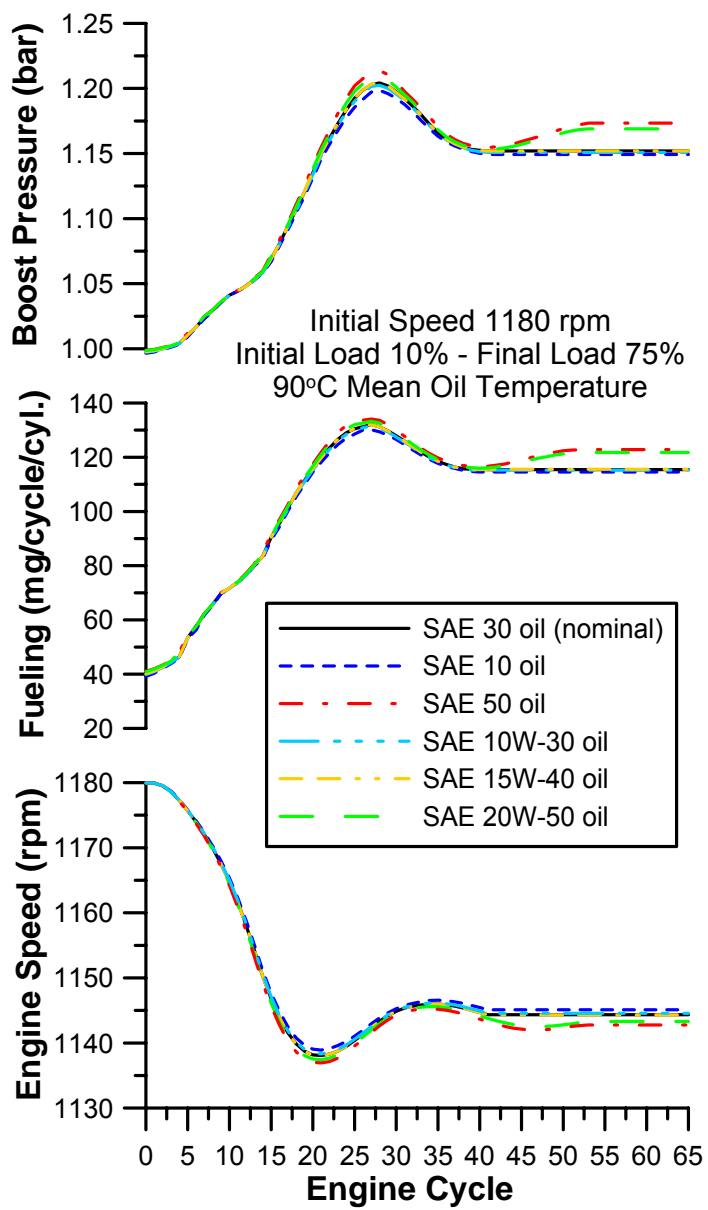
Figure 8
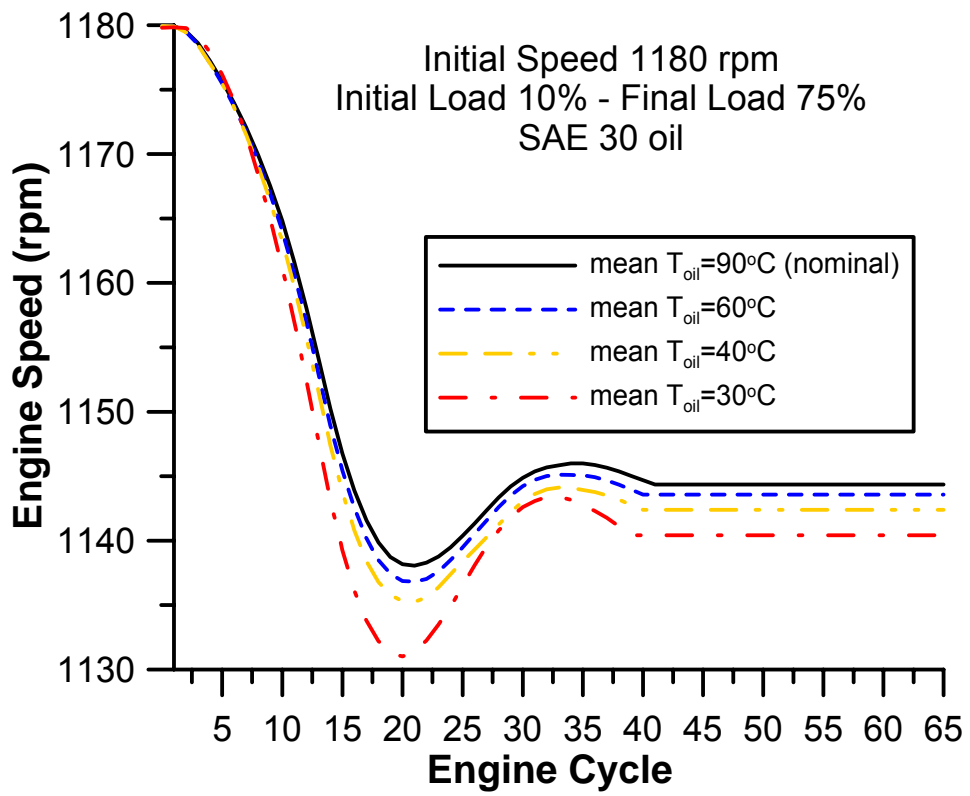
Figure 9
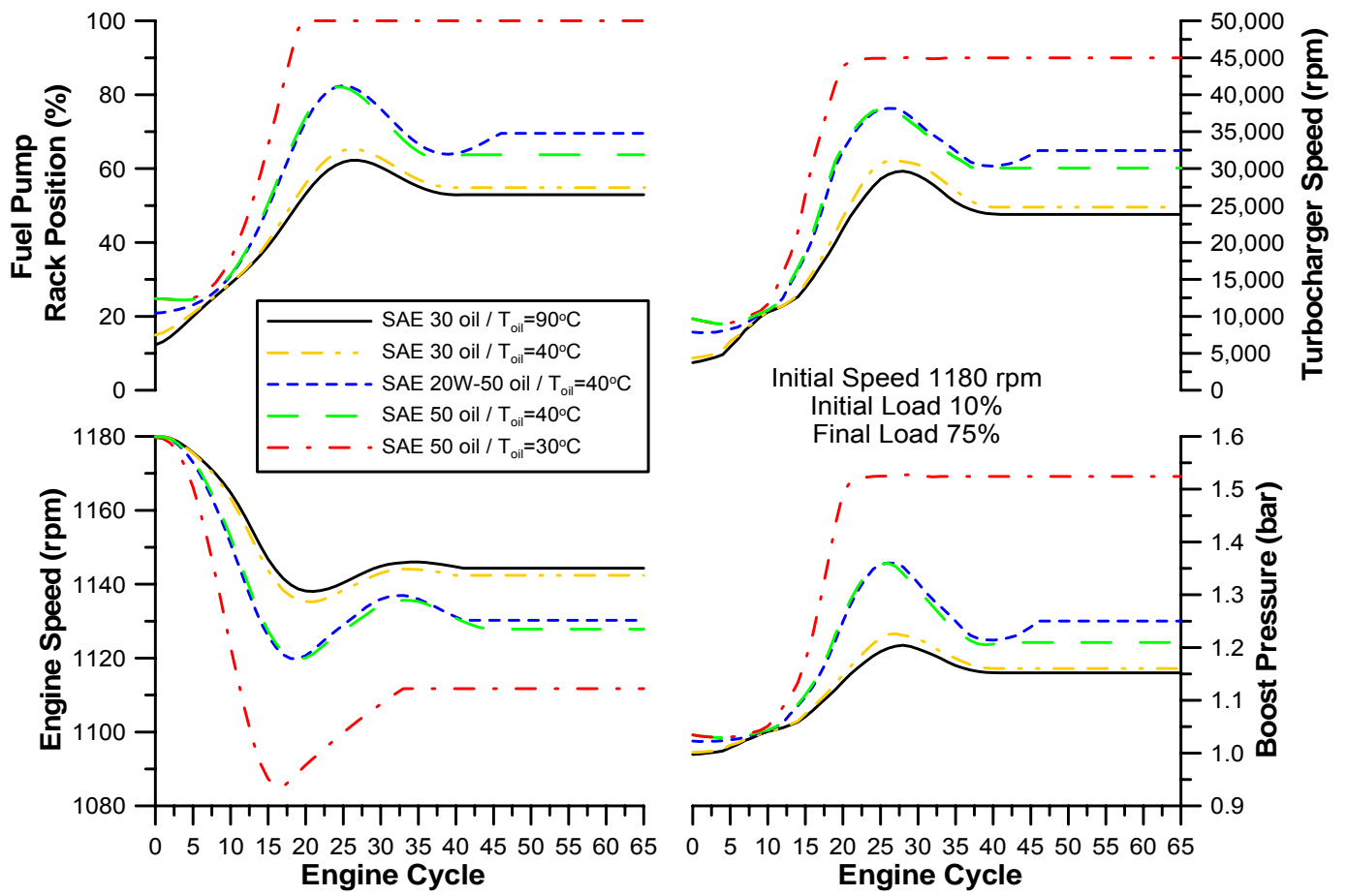
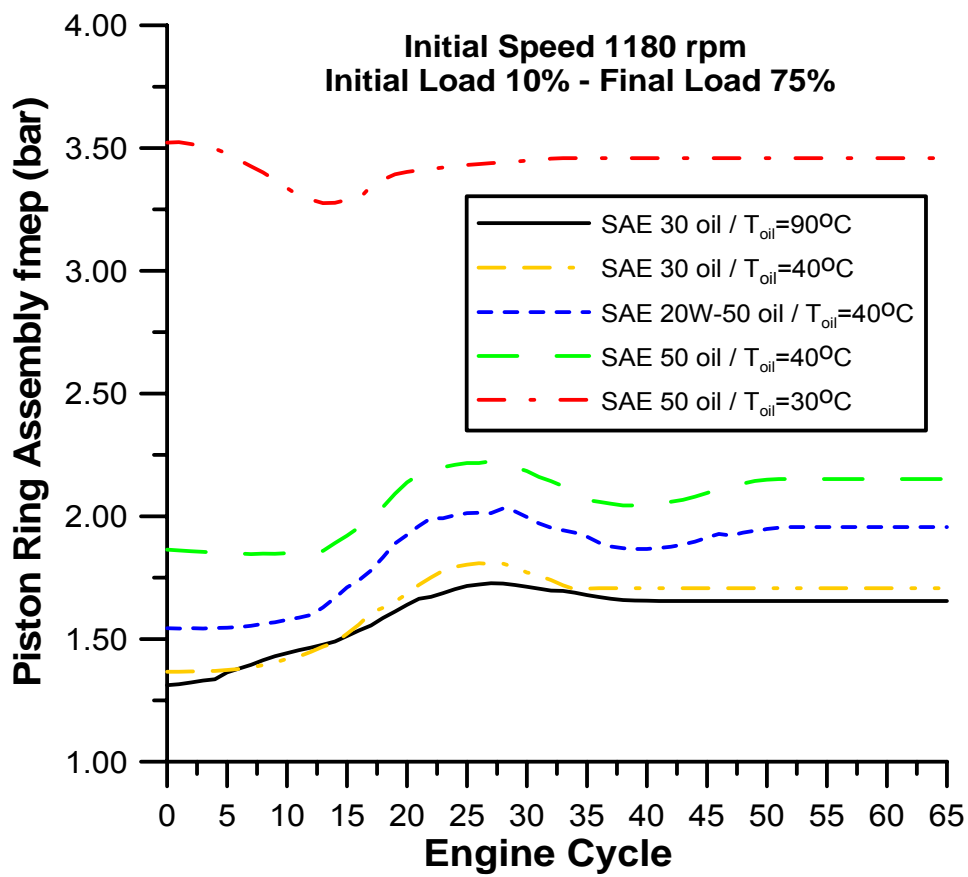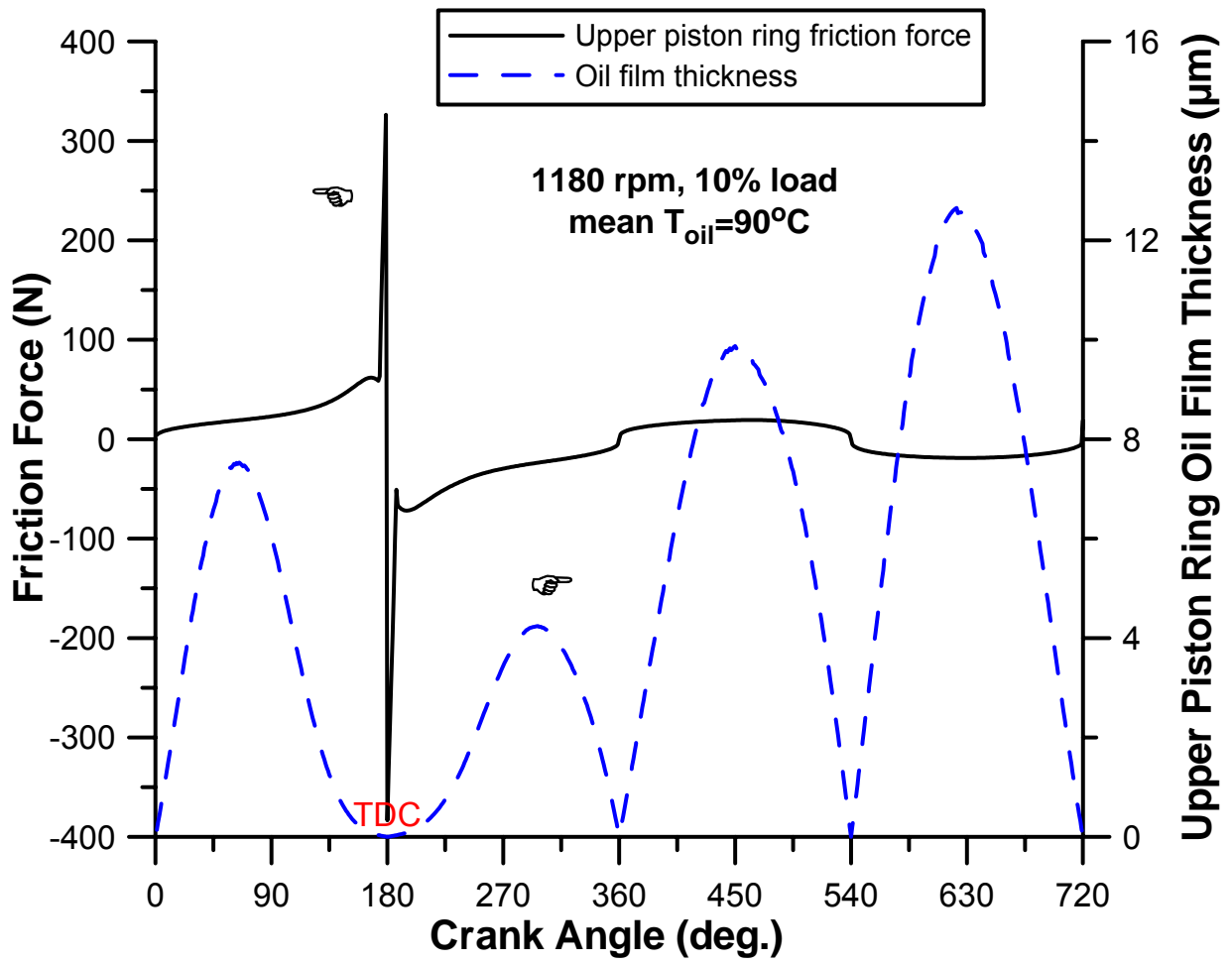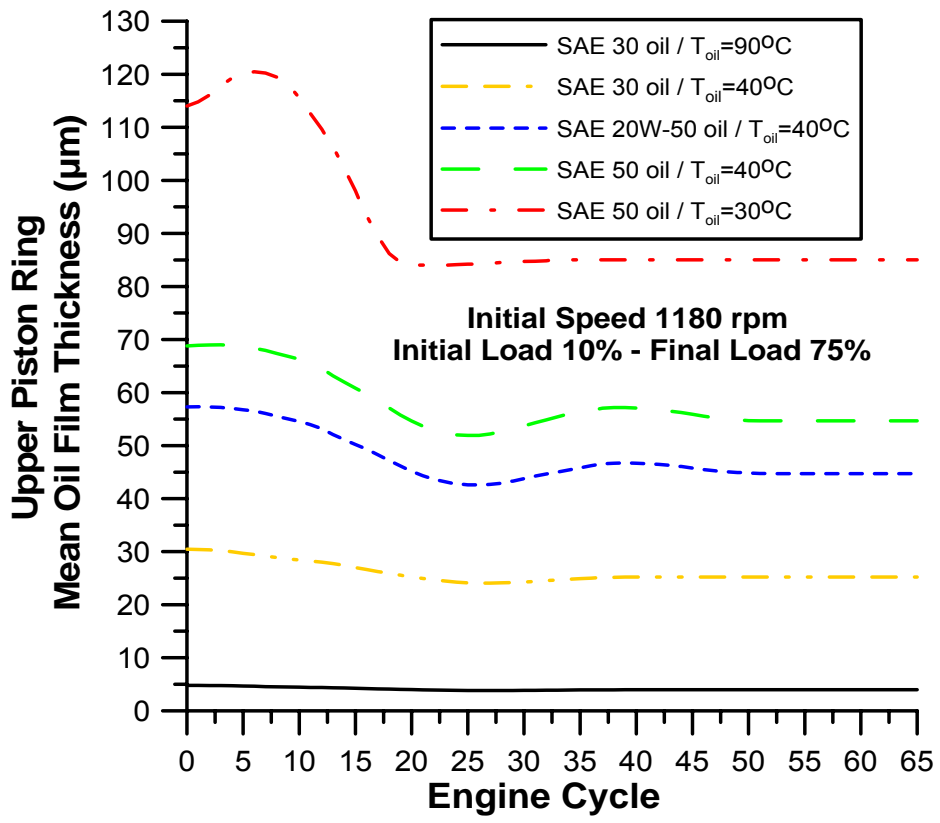**Figure 10**

Figure 11

Figure 12

Figure 13

Table 1: Engine and turbocharger data

Engine Type	4-stroke, 6-cylinder, turbocharged and aftercooled, water-cooled diesel engine
Speed Range	1000÷1500 rpm
Bore / Stroke	140 mm / 180 mm
Connecting Rod Length	350 mm
Maximum Power	236 kW @ 1500 rpm
Turbocharger Moment of Inertia	7.5×10^{-4} kg m^2
Moment of Inertia (engine and load)	15.60 kg m^2

Table 2: Error analysis

	T_{oil}	μ_{oil}	Maximum speed droop	Final speed droop	Relative error in droop max / final
	(^{o}C)	(Ns/m^2)	(%)	(%)	(%)
Nominal (SAE 30 oil)	90	0.01520	3.551	3.020	---
T_{oil}	91	0.01520	3.537	3.014	-0.40 / -0.20
T_{oil}	89	0.01520	3.561	3.025	+0.28 / +0.18
μ_{oil}	90	0.01535	3.569	3.029	+0.51 / +0.31
μ_{oil}	90	0.01504	3.536	3.017	-0.42 / -0.09
T_{oil} / μ_{oil}	91	0.01535	3.560	3.025	+0.25 / +0.17
T_{oil} / μ_{oil}	89	0.01504	3.545	3.014	-0.17 / -0.21